#1

EXPERIMENTAL STUDY OF NONLINEAR DEVICES BY CORRELATION METHODS

L. WEINBERG
L. G. KRAFT

TECHNICAL REPORT NO. 178

JANUARY 20, 1951

RESEARCH LABORATORY OF ELECTRONICS
MASSACHUSETTS INSTITUTE OF TECHNOLOGY
CAMBRIDGE, MASSACHUSETTS

The research reported in this document was made possible through support extended the Massachusetts Institute of Technology, Research Laboratory of Electronics, jointly by the Army Signal Corps, the Navy Department (Office of Naval Research) and the Air Force (Air Materiel Command), under Signal Corps [redacted]

Contract No. DA36-039 sc-100, Project No. 8-102B-0; Department of the Army Project No. 3-99-10-022.

MASSACHUSETTS INSTITUTE OF TECHNOLOGY

RESEARCH LABORATORY OF ELECTRONICS

Technical Report No. 178 January 20, 1951

EXPERIMENTAL STUDY OF NONLINEAR DEVICES BY CORRELATION METHODS

L. Weinberg
L. G. Kraft

Abstract

The correlation technique is applied experimentally to determine the power density spectra of the output of two nonlinear devices, the linear and square-law rectifiers. Curves of the autocorrelation function obtained experimentally for inputs of filtered noise with and without a sine wave are compared with the theoretically calculated curves, and thus an experimental check on some known theoretical results is obtained.

EXPERIMENTAL STUDY OF NONLINEAR DEVICES BY CORRELATION METHODS

Introduction

In the past decade much study has been directed to the mathematical analysis of random noise in communication systems.* Theoretical contributions pertinent to the work described in this report have been made by many investigators, among them Rice (1,2) and Middleton (3,4). Rice's papers present a unified view of the basic methods of noise analysis for both linear and nonlinear circuits. Following his lead Middleton has solved a large number of nonlinear problems of practical importance.

The mathematical analysis is exceedingly complex. There exists, as a consequence, a considerable need for the development of experimental techniques by means of which the important statistical characteristics of random noise in electrical circuits can be determined. These techniques, once developed, can be used for checking existing theoretical results and for the solution of problems not yet susceptible to theoretical analysis. A method that has proved extremely useful in theoretical investigation is the correlation method. This method consists of first finding the autocorrelation function and then by a Fourier transformation of the function determining the power-density spectrum.

There are available in the Research Laboratory of Electronics, M.I.T., an electronic digital correlator (6) for the experimental determination of correlation functions and machines like the electronic differential analyzer (7) and the delay-line filter (8) for accomplishing a Fourier transformation. The correlation method can thus be applied experimentally. Work in this direction was done in 1949 by Knudtzon (9), whose experimental study was confined to linear circuits.

This report extends the range of experimental investigation by the correlation technique to include nonlinear devices, namely, the linear and square-law rectifiers. The first part presents a summary of the pertinent mathematical theory, particular attention being paid to the demonstration of a method which is applicable to the solution of nonlinear circuits. This is the characteristic function method, in which the auto-

---

* For a history of the study see Ref. 5.

correlation function is found through the intermediary of the characteristic function. The second part concerns itself with a discussion of the circuits and experimental technique and a presentation of the results obtained in the form of discrete points which are compared with the theoretically calculated curves.

Part I. Pertinent Statistical Theory

A. Autocorrelation Function, Power Density Spectrum

An important statistical characteristic of a stationary random function such as a noise voltage is its autocorrelation function. If $f_1(t)$ represents the random function, the autocorrelation function $\varphi_{11}(\tau)$ of $f_1(t)$ (10) is given by

$$\varphi_{11}(\tau) = \lim_{T \to \infty} \frac{1}{2T} \int_{-T}^{T} f_1(t) f_1(t + \tau)\, dt. \tag{1}$$

It is often convenient in this report to make use of the normalized autocorrelation function defined as

$$\rho_{11}(\tau) = \frac{\varphi_{11}(\tau)}{\varphi_{11}(0)} = \frac{\lim_{T \to \infty} \frac{1}{2T} \int_{-T}^{T} f_1(t) f_1(t + \tau)\, dt}{\lim_{T \to \infty} \frac{1}{2T} \int_{-T}^{T} f_1^2(t)\, dt}. \tag{2}$$

The following properties of $\rho_{11}(\tau)$ are known:

a. $\rho_{11}(0) = 1$

b. $\rho_{11}(0) \geq |\rho_{11}(\tau)|$

c. $\rho_{11}(\tau)$ is an even function

d. $\rho(\tau) \to 0$ as $\tau \to \infty$ for noise without periodic component and with zero average value.

An important use of the autocorrelation function resides in the fact that the power density spectrum $\Phi_{11}(\omega)$ can be directly obtained from it. Wiener's Theorem relates the two as a Fourier cosine-transform pair. Thus we may write

$$\Phi_{11}(\omega) = \frac{1}{2\pi} \int_{-\infty}^{\infty} \varphi_{11}(\tau) \cos\omega\tau \, d\tau, \tag{3}$$

and

$$\varphi_{11}(\tau) = \int_{-\infty}^{\infty} \Phi_{11}(\omega) \cos\omega\tau \, d\omega. \tag{4}$$

It can be shown (10) that if $f_1(t)$ represents the input to a linear network and $f_2(t)$ the output, as shown in Fig. 1, then

$$\Phi_{22}(\omega) = |H(\omega)|^2 \Phi_{11}(\omega) \tag{5}$$

where $\Phi_{11}(\omega)$ and $\Phi_{22}(\omega)$ are the power density spectra of $f_1(t)$ and $f_2(t)$, respectively, and $H(\omega)$ represents the system function of the network. Of course, no such simple relationship exists for a nonlinear network.

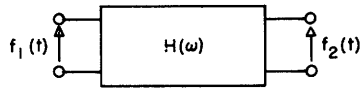

Fig. 1 Representation of linear network.

B. Characteristic Function: Probability Distribution Density, Ergodic Theorem, Moments

A statistical property that is extremely useful in the study of nonlinear circuits is the characteristic function. Preliminary to its definition, some basic definitions must be established. If $y(t)$ represents a stationary random variable and $p(y)\,dy$ is the probability that y lies between y and $y + dy$, then $p(y)$ is called the probability distribution density of the variable y. The average value of y, $\bar{y}$, is

$$\bar{y} = \int y p(y)\, dy, \tag{6}$$

the integral extending over the whole range of possible values of y. The Ergodic Theorem states that the average with respect to the time t of the stationary random variable $y(t)$ is equal to $\bar{y}$, and thus another method is provided for determining $\bar{y}$.

The average of a function of y is given in the same manner, so that

$$\overline{y^n} = \int y^n p(y)\, dy. \tag{7}$$

The averages evaluated by Eq. 7 are called the n^{th} moments of the distribution $p(y)$.

Now the characteristic function can be defined. It is a particular combination of the moments which gives the average value of e^{izy}, where z is a real variable. Letting $\psi(z)$ represent the characteristic function,

we have

$$\psi(z) \equiv \overline{e^{izy}}$$

$$= \overline{\left[\sum_{n=0}^{\infty} \frac{(izy)^n}{n!}\right]}$$

$$= \overline{\left[1 + \frac{izy}{1!} + \frac{(izy)^2}{2!} + \frac{(izy)^3}{3!} + \ldots\right]} \tag{8}$$

$$= 1 + iz\bar{y} + \frac{(iz)^2}{2!}\,\overline{y^2} + \frac{(iz)^3}{3!}\,\overline{y^3} + \ldots.$$

$$= \sum_{n=0}^{\infty} \frac{(iz)^n}{n!}\,\overline{y^n}\,.$$

But the average of e^{izy} is also given by

$$\overline{e^{izy}} = \int e^{izy}\, p(y)\, dy \tag{9}$$

where the integration is carried out for the complete range of values of y, so that we may place infinite limits on the above integral. The right-hand side of Eq. 9 we now recognize as an inverse Fourier transform; thus p(y) is the Fourier transform of the characteristic function, and is therefore determined uniquely by

$$p(y) = \frac{1}{2\pi}\int_{-\infty}^{\infty} \psi(z) e^{-izy}\, dz. \tag{10}$$

Equation 10 represents the first important theorem on the characteristic function. A second important theorem derives from the following: if the characteristic functions of two independent random variables y and x are respectively $\psi(z)$ and $\xi(z)$, then the characteristic function $\zeta(z)$ of the distribution of the sum y + x is given by the product; thus

$$\zeta(z) = \psi(z) \cdot \xi(z). \tag{11}$$

C. Contour Integral Representation of a Nonlinear Device

A useful, often essential artifice for solution of nonlinear problems is the representation of the transfer characteristic of the nonlinear portion of the circuit by a complex integral. For example, if a voltage V is

applied to the input of a nonlinear device, the output current I(V) may be written as an inverse Laplace transform,*

$$I(V) \equiv L^{-1}\left[F(s)\right] \equiv \frac{1}{2\pi i}\int_{C'} F(s)\, e^{sV}\, ds \tag{12}$$

where F(s) is the direct transform

$$F(s) \equiv L\left[I(V)\right] \equiv \int_0^\infty I(V)\, e^{-sV}\, dV \tag{13}$$

and C' is a Bromwich path parallel to the imaginary axis and to the right of all singularities.

The substitution s=iu in Eq. 12 gives

$$I(V) = \frac{1}{2\pi}\int_C F(iu)\, e^{iuV}\, du \tag{14}$$

and changes the path of integration to one along the real axis from $-\infty$ to $+\infty$ with a downward indentation at the origin to avoid a pole or branch point.

D. Fundamental Formula of Characteristic-Function Method

We are now able to demonstrate Rice's derivation** of the fundamental formula of the characteristic-function method for obtaining the output autocorrelation function of nonlinear circuits. Writing Eq. 1 for the output current, we have

$$\varphi_{22}(\tau) = \lim_{T\to\infty} \frac{1}{2T}\int_{-T}^{T} I(t)\; I(t+\tau)\, dt. \tag{15}$$

Substituting Eq. 14 and rearranging give

$$\varphi_{22}(\tau) = \frac{1}{4\pi^2}\int_C F(iu)\, du \int_C F(iv)\, dv \lim_{T\to\infty}\frac{1}{2T}\int_{-T}^{T} \exp\left[iuV(t) + ivV\,(t+\tau)\right] dt. \tag{16}$$

The limit in the above equation is recognized as the characteristic function of the distribution of the sum of two random variables, V(t) and $V(t+\tau)$. Denote this characteristic function by $g(u, v; \tau)$. Then,

$$\varphi_{22}(\tau) = \frac{1}{4\pi^2}\int_C F(iu)\, du \int_C F(iv)\, g(u, v; \tau)\, dv \tag{17}$$

---

* Ref. 1, Appendix 4A, p. 149. Other transforms may be used.

** Ref. 1, p.136, Eq. 4.8-6.

which is the fundamental formula of the characteristic-function method. It remains to evaluate the above integral and its Fourier cosine transform,

$$\Phi_{22}(\omega) = \frac{1}{2\pi}\int_{-\infty}^{\infty} \varphi_{22}(\tau)\cos\omega\tau \, d\tau, \tag{18}$$

to obtain the power density spectrum of the output current I.

Part II. Experimental Study

A. Circuit Details

A block diagram of the essential components used in the experimental procedure is shown in Fig. 2. White noise is by definition noise that has a uniform power-density spectrum over a frequency range that is large compared to the range of interest, which in this experiment is the filter bandwidth. The source of white noise employed a 6D4 gas triode as the primary noise generator.* Monitoring of the rectifier input and the rectifier bias voltages was accomplished by use of the thermocouple and d-c meters, respectively.

The band-pass filter, the amplifier, and the nonlinear element were incorporated in one chassis. From the circuit diagram in Fig. 3, it is seen that the filter is a simple RLC parallel-tuned circuit, whose Q may be varied in steps by use of the ganged switch. This switch varies both series and parallel resistance, in order to provide approximately constant voltage across the tuned circuit for the different Q's. Tapping the condenser of the tuned circuit serves the dual purpose of impedance transformation and voltage step-up.

After linear amplification of the filtered random noise by the first three tubes, the noise is fed to a cathode follower, which serves as a low internal resistance voltage source for the nonlinear element. The cathode resistances in the amplifier stages are unby-passed for increased linearity of amplification. When a noise plus a sine-wave input was desired, an oscillator was connected through an appropriate RC-combination to the plate of tube V-3.

The negative 150-volt connection to the resistance in the cathode-follower circuit is used to cancel the positive direct voltage developed

*Equipment designed by C. A. Stutt. See Ref. 11 for circuit diagram.

across the cathode resistance. Thus the net direct voltage across the nonlinear element can be adjusted to give zero bias. For the linear rectifier a 9005 tube was found satisfactory. A series connection of eight 1N48 diodes and a 100-ohm resistor was substituted for the 9005 and its load resistance to provide an approximately square-law characteristic. Fig. 4 shows a plot on log-log coordinates of the measured points of the characteristic.

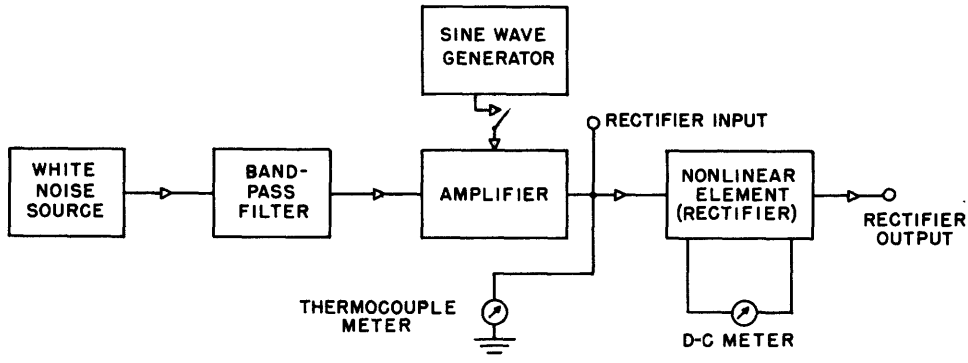

Fig. 2 Block-diagram representation of circuit.

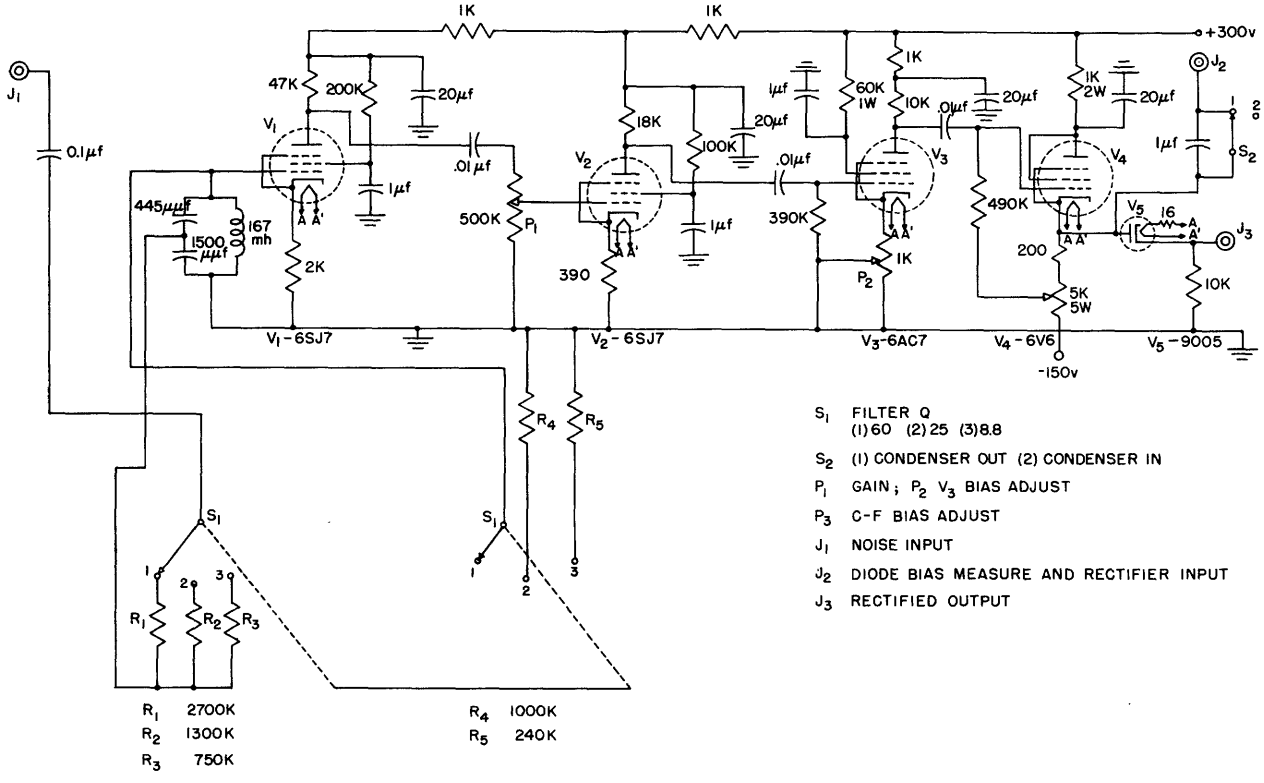

Fig. 3.

B. Experimental Procedure

The resonant frequency of the band-pass filter was 23 kc/sec, and the sine-wave generator was set to this frequency. Autocorrelation curves of the rectifier input, with and without the sine-wave present, were obtained for three Q-values (60,25,8.8) of the resonant circuit. Autocorrelation curves of the rectifier output were obtained for each of the above inputs. The two rectifiers, the linear 9005 tube and the square-law 1N48 crystal diodes, were studied in this way.

In obtaining each point of the correlation curve, the digital correlator obtains pairs of samples of the amplitude of the voltage waveform, multiplies the members of each pair and sums many such products. Approximately 31,000 pairs of samples were obtained over a period of about one minute of the signal for each point plotted on the short curves shown in Fig. 8. Approximately 62,000 pairs of samples over a two-minute period of signal were obtained for each point of the three long curves. The τ-range of the curves is 0-218 μsec, or 0-436 μsec, as indicated on the curves.

During the course of obtaining the correlation curves, it became apparent that it was possible to alter the correlator itself to accomplish the rectification function of the 9005 tube or of the 1N48 diodes. This is done by causing the number-generating part of the digital correlator to limit at the rectification level desired. In particular, the high speed counter of the number generator was arranged so that it stopped at the half full level. This corresponds to biasing the rectifiers at zero voltage. The last curve on page 16 and the last three curves on page 17 were obtained in this manner. In the square-law case, the circuit of Fig. 5 produced "squaring" of the filtered noise while the correlator accomplished rectification.

C. Calculations from the Theory

As regards the symbolism used in this section, the subscript 1 and subscript 2 will signify input and output, respectively, and when it is necessary to separate the input into components, subscript n will refer to

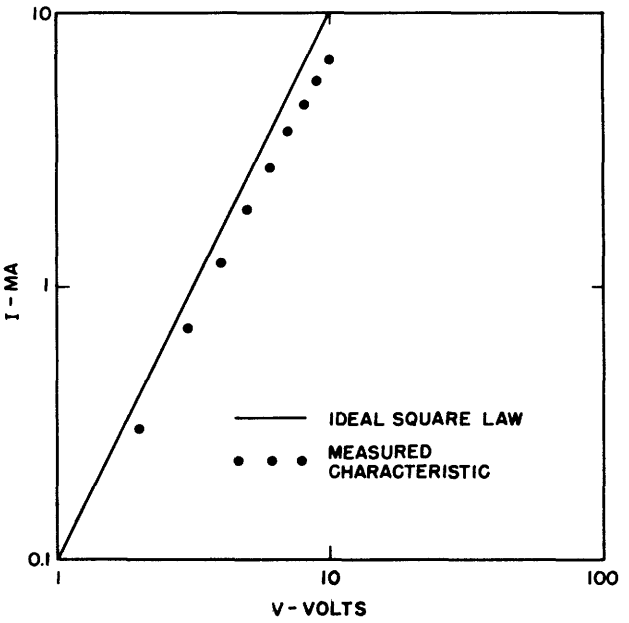

Fig. 4 Volt-ampere characteristic of square-law rectifier (log-log coordinates).

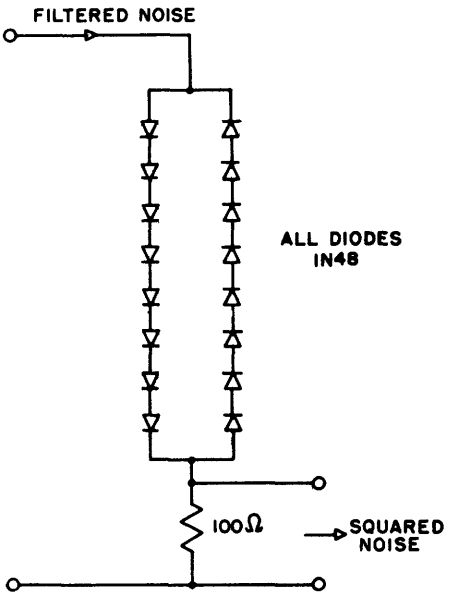

Fig. 5 Circuit for squaring input voltage.

Fig. 6 Simplified circuit diagram with V_n = filtered random noise of center frequency ω_0; $V_s = P \cos \omega_0 t$.

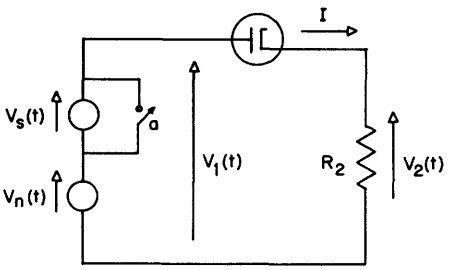

noise and s to sinuisoidal signal. It is believed that no confusion should result from the repeated use of the same symbol, e.g. $\rho_{22}(\tau)$ for the normalized autocorrelation function of different outputs, since it will be clear from the context to which output reference is being made.

The basic circuit of this experiment can be reduced to the one shown in Fig. 6. When the input is noise alone, switch "a" is closed.

First we will obtain the autocorrelation functions of the input to the rectifier. The calculations require merely an application of linear theory. The filtered noise input to the rectifier, V_n, is itself the output of the RLC band-pass filter with a white noise input. Let the uniform power spectrum of this input be $\Phi_{11}(\omega) = a^2$; then, in accordance with Eq. 5

$$\Phi_{nn}(\omega) = |Z(\omega)|^2 \Phi_{ii}(\omega)$$

$$= \frac{L^2\omega^2 a^2}{\left[1 - \left(\frac{\omega}{\omega_o}\right)^2\right]^2 + \frac{\omega^2}{Q^2\omega_o^2}} \tag{19}$$

where

$Z(\omega)$ = impedance of the tuned circuit,

$$\omega_o = \frac{1}{\sqrt{LC}}$$

and

$$Q = \frac{R}{\omega_o L} = R\omega_o C.$$

The autocorrelation function is obtained by use of Eq. 4, and is found to be (11)

$$\varphi_{nn}(\tau) = \frac{\pi a^2 L^2 \omega_o^3 Q}{2} e^{\frac{-\omega_o|\tau|}{2Q}} \cos\left(\omega_o\tau + \frac{1}{2Q}\right) \tag{20}$$

$$\approx \frac{\pi a^2 L^2 \omega_o^3 Q}{2} e^{\frac{-\omega_o|\tau|}{2Q}} \cos\omega_o\tau$$

where the approximation holds for high-Q circuits. Hence the normalized autocorrelation function is simply

$$\rho_{nn}(\tau) = e^{\frac{-\omega_o|\tau|}{2Q}} \cos\omega_o\tau. \tag{21}$$

Since the autocorrelation function for the sinusoidal voltage, $V_s = P\cos\omega_o t$, is

$$\varphi_{ss}(\tau) = \frac{P^2}{2}\cos\omega_o\tau \tag{22}$$

the autocorrelation function for the total input, $V_n + V_s$, to the rectifier and load is

$$\varphi_{ii}(\tau) = \varphi_{nn}(\tau) + \varphi_{ss}(\tau)$$

$$= Ae^{\frac{-\omega_o|\tau|}{2Q}} \cos\omega_o\tau + \frac{P^2}{2}\cos\omega_o\tau. \tag{23}$$

In Eq. 23 we have made use of the fact that the noise and sinusoidal voltages are unrelated so that the cross-product terms are zero.

Now, in turning our attention to the output, let us consider first the more difficult case of determining the output autocorrelation function for the noise plus sine-wave input. We know by Eq. 11 that the characteristic function of $V_1(t)$ is equal to the product of the characteristic functions of its two components. Thus

$$g(u,v;\tau) = g_s(u,v;\tau) \cdot g_n(u,v;\tau). \tag{24}$$

The evaluation of $g_s(u,v;\tau)$ proceeds more easily on the basis of the time average, which by the Ergodic Theorem is equivalent to the average obtained through the use of the probability distribution. The time average is

$$g_s(u,v;\tau) = \lim_{T\to\infty} \frac{1}{T} \int_0^T \exp\left[i P \left(u \cos \omega_o t + v \cos \omega_o\{t + \tau\}\right)\right] dt \tag{25}$$

which Rice has shown yields

$$g_s(u,v;\tau) = J_o\left(P\sqrt{u^2 + v^2 + 2uv \cos \omega_o\tau}\right). \tag{26}$$

The characteristic function for the noise can be shown to be*

$$g_n(u,v;\tau) = \exp\left[-\frac{\varphi_{nn}(0)}{2}(u^2 + v^2) - \varphi_{nn}(\tau)uv\right]. \tag{27}$$

Therefore the output autocorrelation function, obtained by substitution of Eqs. 26 and 27 in Eq. 17 is

$$\varphi_{22}(\tau) = \frac{1}{4\pi^2} \int_C F(iu) e^{-\frac{\varphi_{nn}(0)}{2}u^2} du \int_C F(iv) e^{-\frac{\varphi_{nn}(0)}{2}v^2 - \varphi_{nn}(\tau)\,uv}$$

$$\times J_o\left(P\sqrt{u^2 + v^2 + 2uv \cos \omega_o\tau}\right) dv. \tag{28}$$

We can now specify the nonlinear device so that the Fourier transform $F(iu)$ can be determined. For the linear rectifier, where the output current is

$$I = \begin{cases} \alpha V & V \geq o \\ o & V < o \end{cases} \tag{29}$$

the Laplace transform $F(s)$** is $\frac{\alpha}{s^2}$, so that $F(iu) = \frac{-\alpha}{u^2}$.

---

*Ref. 1, p. 135, Eq. 4.8-3.

**Ref. 12, Appendix A, Transform 2.101.

Similarly, for a square-law rectifier with the characteristic

$$I = \begin{cases} \alpha V^2 & V \geq 0 \\ 0 & V < 0 \end{cases} \tag{30}$$

the transform* is $F(iu) = \dfrac{2\alpha i}{u^3}$.

Eq. 28 has not been evaluated in closed form, but by use of the expansion

$$J_o\left(P\sqrt{u^2 + v^2 + 2uv\cos\omega_o\tau}\right) = \sum_{m=0}^{\infty} \varepsilon_m (-1)^m J_m(Pu) J_m(Pv) \cos m\omega_o\tau \tag{31}$$

in which $\varepsilon_o = 1$, $\varepsilon_m = 2$ for $m \geq 1$; and by expanding $\exp\left[-\varphi_{nn}(\tau)uv\right]$ into the infinite series for an exponential, Rice has obtained the following double series

$$\exp\left[-\varphi_{nn}(\tau)uv\right] J_o\left(P\sqrt{u^2 + v^2 + 2uv\cos\omega_o\tau}\right) \tag{32}$$

$$= \sum_{m=0}^{\infty} \sum_{k=0}^{\infty} (-1)^{m+k} \varepsilon_m \cos m\omega_o\tau \frac{\left[\varphi_{nn}(\tau)\, uv\right]^k}{k!} J_m(Pu)\, J_m(Pv).$$

This double summation separates the variables so that the integration is somewhat simplified. With the aid of Eq. 32 the repeated integral in Eq. 28 reduces to the form

$$\varphi_{22}(\tau) = \sum_{m=0}^{\infty} \sum_{k=0}^{\infty} \frac{1}{k!} \varphi_{nn}^k(\tau)\, h_{mk}^2\, \varepsilon_m \cos m\omega_o\tau \tag{33}$$

in which

$$h_{mk} = \frac{i^{m+k}}{2\pi} \int_C F(iu)\, u^k\, J_m(Pu)\, e^{-\left(\frac{\varphi_{nn}(0)\, u^2}{2}\right)} du. \tag{33a}$$

Rice**has shown that for the linear rectifier

$$h_{mk} = \frac{\alpha \left(\frac{\varphi_{nn}(0)}{2}\right)^{\frac{1-k}{2}} \frac{x^{\frac{m}{2}}}{m!}}{2\,\Gamma\left(\frac{3-k-m}{2}\right)} \; {}_1F_1\left(\frac{k+m-1}{2}\,;\; m+1;\; -x\right) \tag{34}$$

---

* Ref. 12, Appendix A, Transform 2.102.

**Ref. 1, p. 144, Eq. 4.10-5

and for the square-law rectifier

$$h_{mk} = \frac{\alpha \left(\frac{\varphi_{nn}(0)}{2}\right)^{\frac{2-k}{2}} \frac{m}{2}}{2\,\Gamma\left(\frac{4-k-m}{2}\right)} \frac{x}{m!}\; {}_1F_1\left(\frac{k+m-2}{2}\,;\; m+1;\; -x\right) \tag{35}$$

where $x = \dfrac{\text{sine wave power}}{\text{noise power}} = \dfrac{P^2}{2\varphi_{nn}(0)}$

and ${}_1F_1$ is the confluent hypergeometric function. Values of $x = \frac{1}{2}$ and $x = 1$ were used in the experiment.

When the input to the linear rectifier is filtered noise only, the autocorrelation function for the output is*

$$\varphi_{22}(\tau) = \frac{\alpha^2 \varphi_{nn}(0)}{2\pi}\left\{\left[1 - \rho_{nn}^2(\tau)\right]^{\frac{1}{2}} + \rho_{nn}(\tau)\,\cos^{-1}\left[-\rho_{nn}(\tau)\right]\right\} \tag{36}$$

where

$$\rho_{nn}(\tau) = \frac{\varphi_{nn}(\tau)}{\varphi_{nn}(0)} = e^{-\frac{\omega_o|\tau|}{2Q}}\cos\left(\omega_o\tau + \frac{1}{2Q}\right)$$

and the arc cosine is taken between o and π.

For the square-law rectifier with a filtered noise input, Middleton has shown that**

$$\varphi_{22}(\tau) = \frac{\alpha^2 \varphi_{nn}(0)}{2\pi}\left\{\cos^{-1}\left[-\rho_{nn}(\tau)\right]\left(1 + 2\rho_{nn}^2(\tau)\right) + 3\rho_{nn}(\tau) \times \left(1 - \rho_{nn}^2(\tau)\right)^{\frac{1}{2}}\right\} . \tag{37}$$

D. Experimental Results

The autocorrelation function is recorded by the digital correlator in two forms. A multiple pen Esterline-Angus Recorder records a number in binary-digital form for each τ-step. An example of such a record is shown in Fig. 7. The second form of recording is made by a General Electric Recording Microammeter; this record gives an immediate visual check on

---

* Ref. 1, p. 133, Eq. 4.7-5; Ref. 3, p. 793, Eq. 4-13 is equivalent.

** Ref. 4, p. 480, Eq. 78.

Fig. 7 Output autocorrelation function recorded in binary-digital form (Q=8.8, linear rectifier, noise input).

results. Photographs of the autocorrelation curves for the different inputs and Q-values, as given in the second form of recording, are shown in Fig. 8.

The theoretically determined autocorrelation curves identified in Figs. 9 through 14 were plotted for a τ-range of 136μsec ($\omega_o\tau$-range of 1080°). For convenience each theoretical curve is normalized with respect to its value at τ=0.

Presented on the same sheets with the theoretical plots are the discrete points obtained from the experimental data. When two sets of experimental data were obtained for one curve, the average was used. To plot the experimental points from the binary-digital data, it was necessary to perform a subtraction to obtain the zero level and a multiplication to obtain a good fit, as determined by visual inspection. An illustration of this procedure is the following: suppose we have obtained an exponentially damped cosine autocorrelation curve for Q=60, whose digital data show that the τ=0 value is 154, the next maximum is 150, and the first minimum occurs at the half cycle and is 120. For the high-Q case the damping of the cosine is approximately linear for the first cycle so that the envelope would decrease to 152 at the half-cycle point. The zero value can then be obtained as $(152 + 120)/2 = 136$. This value is then subtracted from the number representing each point and the resulting values normalized for a good fit. Suppose, after inspection, it is felt that allowing the τ=0 value to be 1 gives a good fit to the theoretical curve. Then,

$$(154 - 136)X = 1, \quad X = \frac{1}{18} = 0.0556$$

is the appropriate normalizing factor.

Figures 12 and 14 show output autocorrelation functions of rectified noise plus sine wave which take on negative values. The reason for this is that the d-c term in the series (m = o, k = o) of Eq. 33 has been omitted in the computation.

A Fourier transformation of the curve shown in Fig. 15.1 was obtained on the electronic differential analyzer; a photograph of the result is shown in Fig. 15.2. A Fourier transform of the curve of Fig. 16.1 was obtained on the delay-line filter; a plot of the resulting power density spectrum is shown in Fig. 16.2.

An error is to be expected due to the finite number of samples measured by the correlator. In general, such an error depends on the number of samples, the statistical properties of the signal measured, and the large d-c level inserted by the correlator. For the case of large τ, where the samples are nearly independent, it can be shown that the ratio of the rms error (σ_e) to the variance (σ^2) of $f_1(t)$, the signal under study, is

$$\frac{\sigma_e}{\sigma^2} = \sqrt{\frac{1}{N} + \frac{2\left[D + \overline{f_1(t)}\right]^2}{N\sigma^2}} \tag{38}$$

where N = number of samples averaged

$\overline{f_1(t)}$ = average of signal under study

D = constant added to $f_1(t)$ by the correlator .

The quantities in the equation may be determined from the autocorrelation curve itself. For example, the autocorrelation curve shown in Fig. 15.1 was obtained with the number of samples $N = 31 \times 2^{11}$, and the values of σ^2 and $\left[D + \overline{f_1(t)}\right]^2$ may be obtained from the experimental data as

$$\sigma^2 = 3.23 \times 2^{11}$$

$$\left[D + \overline{f_1(t)}\right]^2 = 101.7 \times 2^{11} .$$

Therefore

$$\frac{\sigma_e}{\sigma^2} \approx 0.032.$$

Approximately one-third of the measured values might be expected to fall outside $\pm \sigma_e$ which equals ± 0.02 on the normalized curve shown. This agrees very well with the observed results.

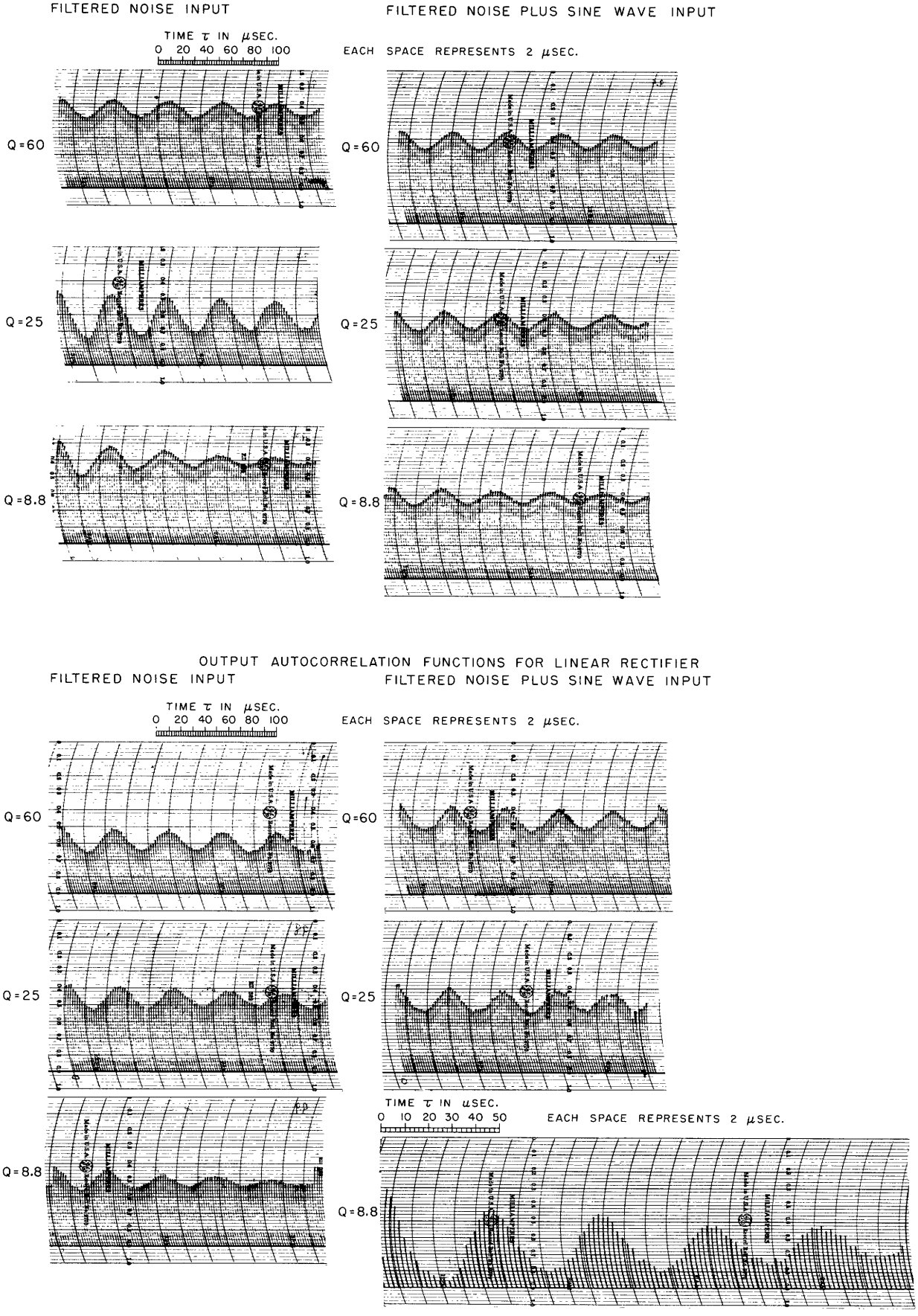

Fig. 8 Autocorrelation functions as recorded by correlator.

OUTPUT AUTOCORRELATION FUNCTIONS FOR SQUARE-LAW RECTIFIER
FILTERED NOISE INPUT

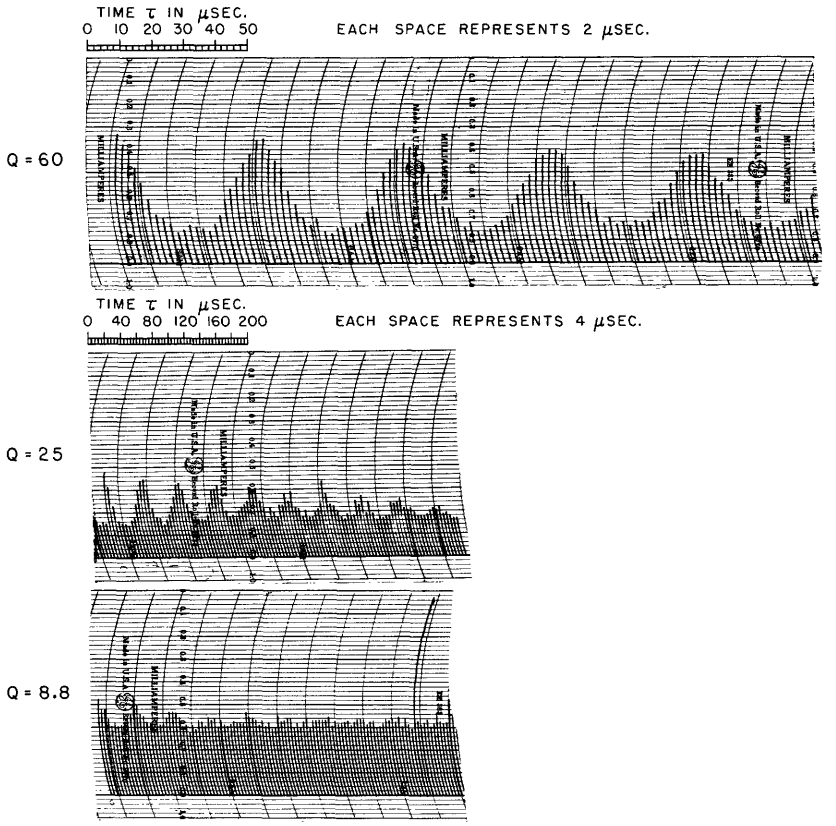

OUTPUT AUTOCORRELATION FUNCTIONS FOR SQUARE-LAW RECTIFIER
FILTERED NOISE PLUS SINE WAVE INPUT

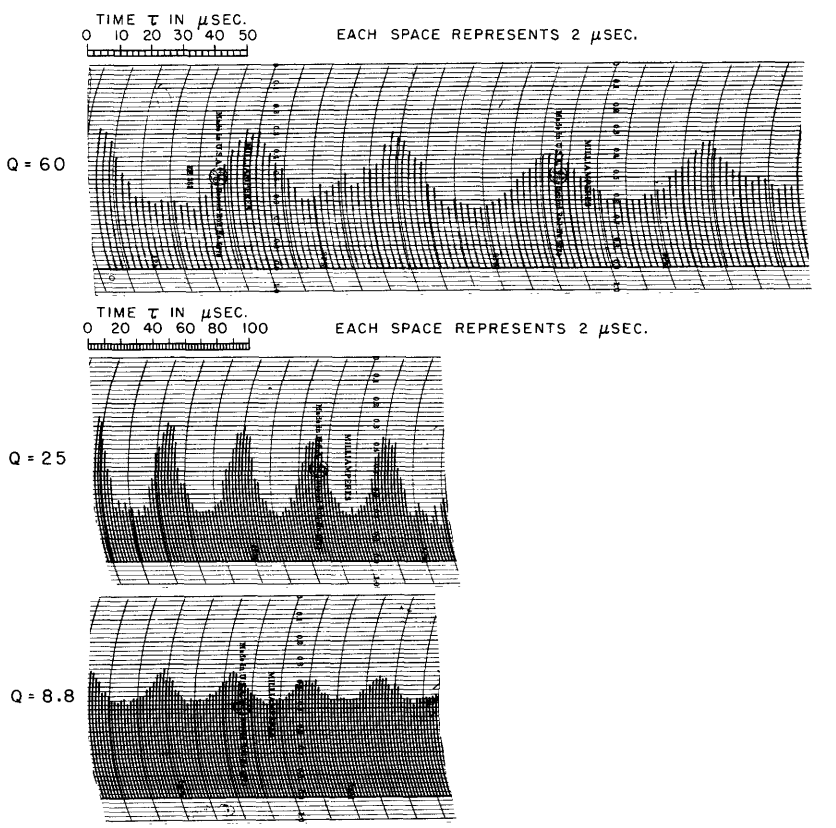

Fig. 8 (cont'd) Autocorrelation functions as recorded by correlator.

There are errors other than that due to the finite number of samples. Causes of the most important errors seemed to be:

1. amplitude drift in the sampling circuits of the correlator
2. voltage drift in the power supplies used with the noise filtering and amplifying devices
3. departure of the rectifiers from the idealized versions.

When a sine wave was added to the noise, additional errors are caused by:

4. amplitude drift in sine-wave generator
5. synchronization of the sine-wave oscillator with the sampling frequency of the correlator.

In order to reduce errors of measurement in the sampling circuits of the correlator, a second compensator was added so that each channel of the machine is now compensated separately (6). This was done after only a few of the tests for this report, and all curves which had already been obtained were discarded. The compensators act to keep the median value of the measured samples at a constant level. That is, the compensators provide a correction in the number-generating circuits which tends to stabilize the median value of the binary numbers used in the digital parts of the machine. The effectiveness of the compensators depends on the statistical properties of the input signal; signals with a well defined median value are handled best. For the results in this report, the effects of drift originally present in the measuring portions of the correlator were reduced to negligible values compared with errors due to other causes. Some of the curves, when inspected closely, will indicate the magnitude of the drifts still present.

Changes in the power supply voltages and the signal levels from the noise and sine-wave generators were made small by constant monitoring and manual adjustment. A few minor circuit modifications were made to reduce the effects of such changes.

The departure of the rectifiers from ideal is an unavoidable part of the experimental method. However, the use of the correlator itself to perform the rectifying function of the diodes, as mentioned above, is a way of decreasing the errors introduced. Since results obtained using either the diodes or the correlator agree well with the theoretical curves, such errors do not seem to have been important.

The effects of synchronization of the input voltage periodicities with the sampling period of the correlator are of importance. The correlator obtains samples of the input signal and multiplies each sample by a second sample taken a time τ later. The products of a great number of sample pairs are added together to obtain one value of the correlation curve before shifting to a new value of τ. If the sampling takes place in synchronism with a periodic input signal, it can be seen that the first samples will always have the same value (depending only on the phase of sampling). Likewise, the samples obtained τ seconds later will be constant for any one value of τ, and will depend on the phase of the input signal at which the second sample is being taken. The result of multiplying the second sample by the first and adding many such products is the average value of the second sample multiplied by a large constant. As τ is changed, the average value for each corresponding phase is obtained and the output curve of the correlator then has the same shape as the periodic waveform at the input. This difficulty can be met by setting the frequency of the input signal at a value different from any integral multiple of the sampling frequency. This was done during this experiment, and frequent observations made to correct the oscillator frequency for drifts.

It has been suggested that the inherent difficulty present in the correlator due to constant frequency of sampling may be avoided by sampling at random intervals. This appears to be an excellent suggestion for correlators designed for inputs of a periodic nature.

The compensators produce a further difficulty when the input signal frequency is a harmonic of the sampling rate. Whenever the samples of input voltage obtained by the correlator have constant magnitude, the compensators will adjust the number-generating portions of the machine to produce the constant median number for the constant magnitude of sample. If the input samples change to another constant level, the compensators adjust again so that the same median number results, and no change appears in the correlation curve. Since the compensators make such an adjustment in a few seconds (time constant ≈ 4 sec), the input signal frequency should differ by a few cycles per second from any harmonic of the sampling rate. This effect was detected by observing the compensator voltages. When the signal frequency drifted near a harmonic of the sampling rate, these voltages would oscillate as the compensators followed the slow difference frequency.

E. Conclusions

The autocorrelation method has been applied experimentally to the determination of power density spectra for the output of some nonlinear devices. The results for the autocorrelation functions have been compared with the theoretically calculated curves. It may be stated that an experimental check on some known theoretical results has been obtained, and it is hoped that the technique will be extended to the investigation of nonlinear problems that have not yet been solved analytically.

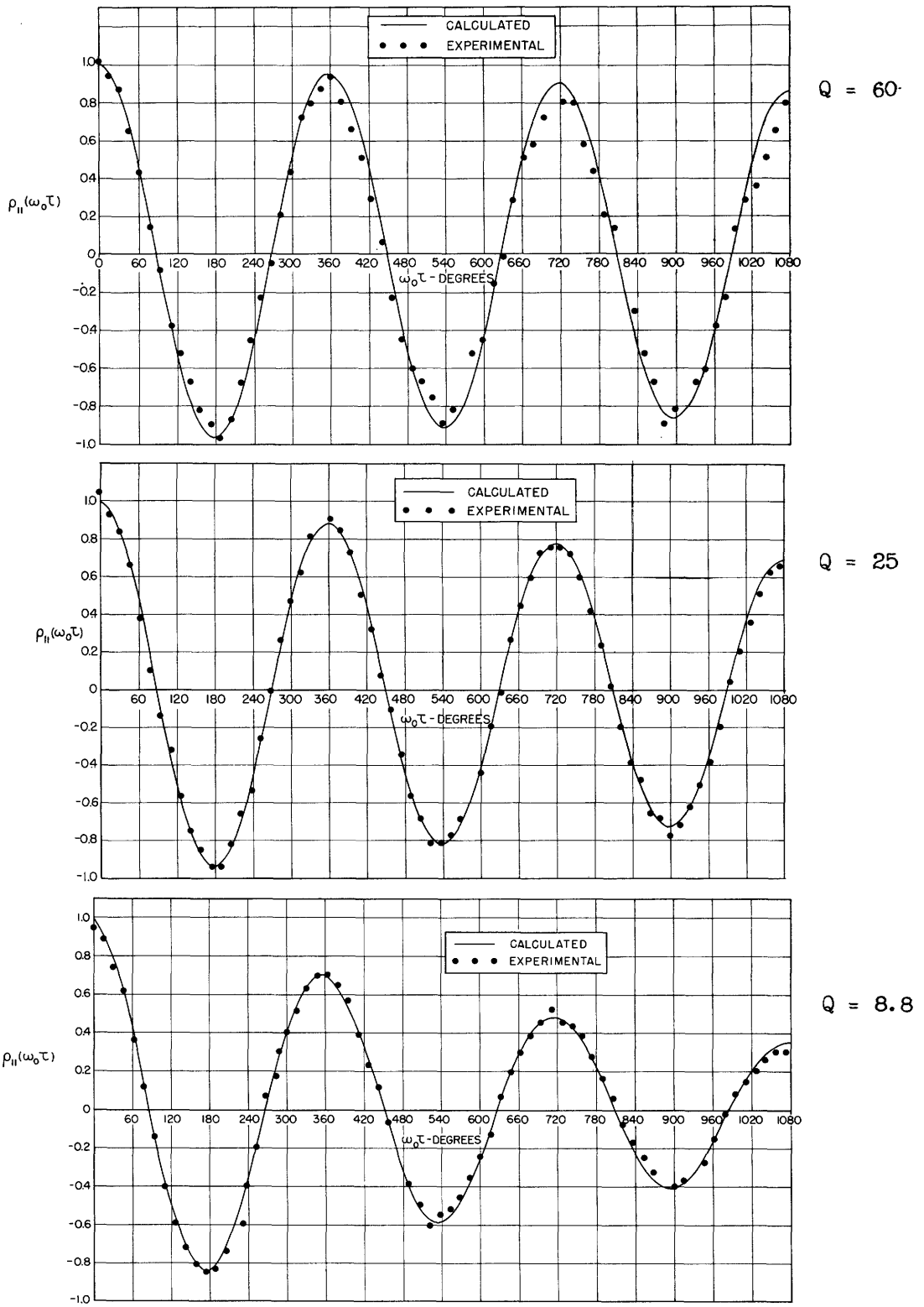

Fig. 9 Normalized input autocorrelation functions $\rho_{11}(\omega_0\tau)$ for filtered noise input [see Eq. (21)].

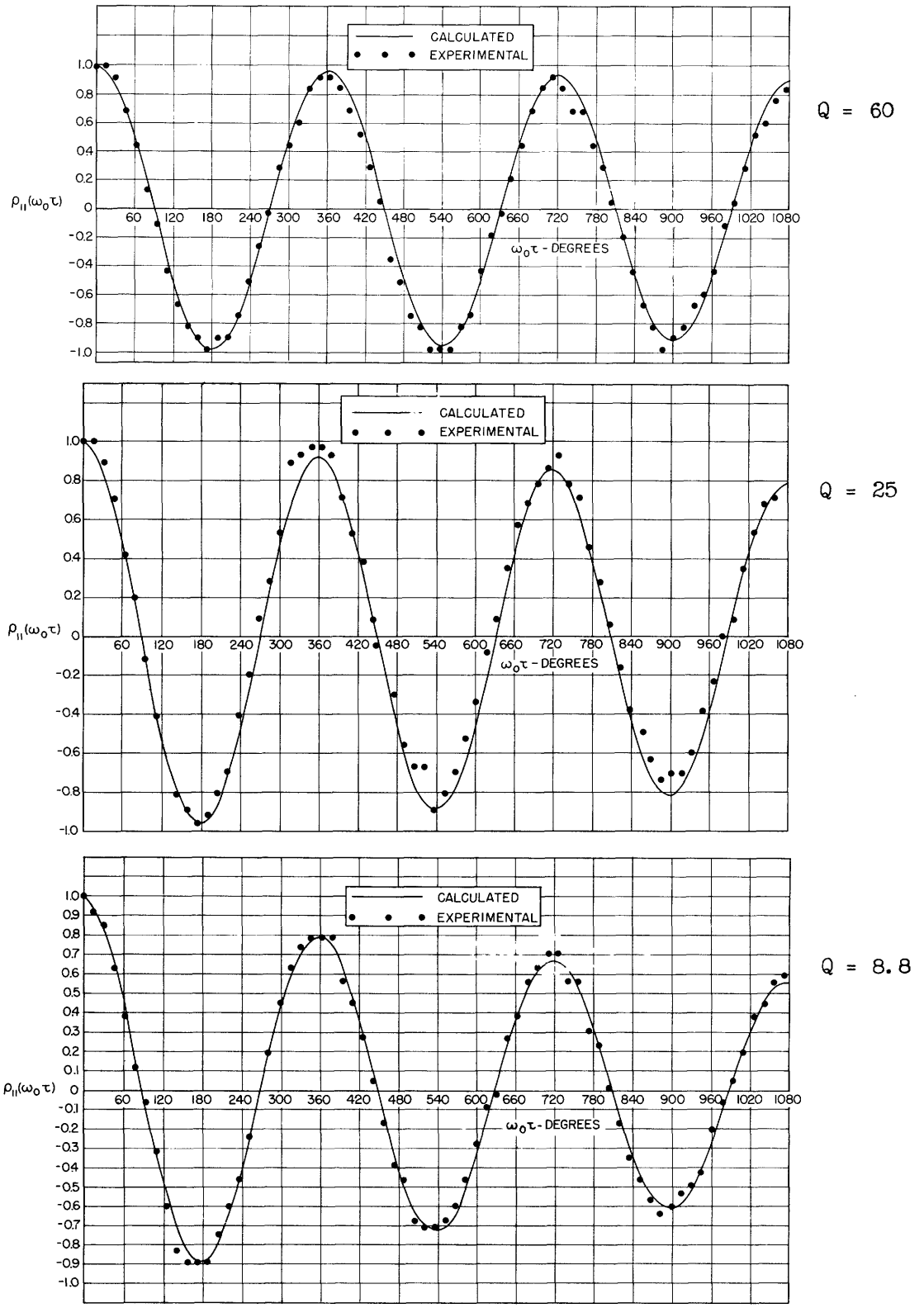

Fig. 10 Normalized input autocorrelation functions $\rho_{11}(\omega_0\tau)$ for filtered noise plus sine wave input [see Eq. (23)].

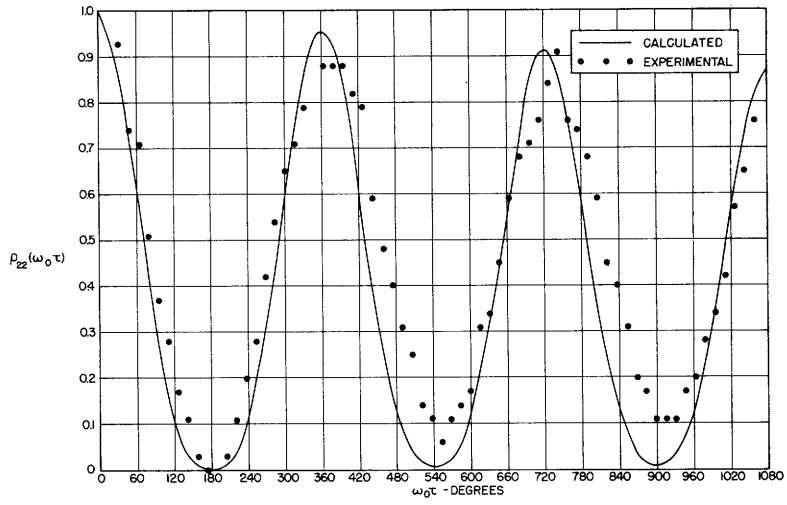

Q = 60

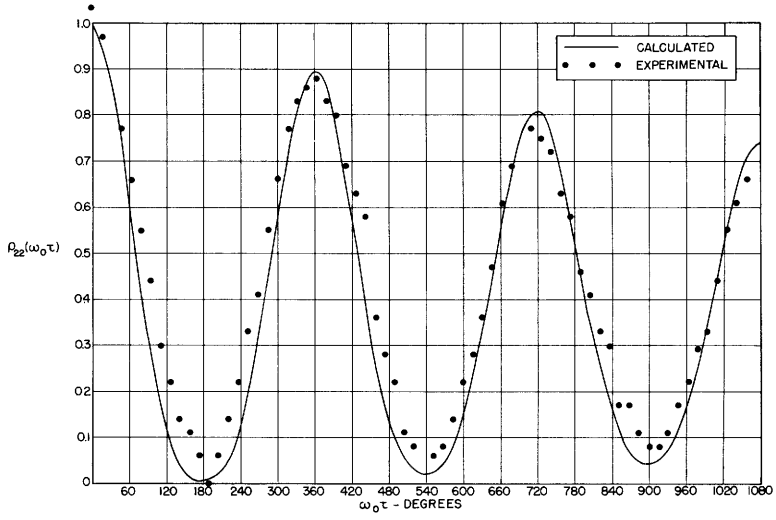

Q = 25

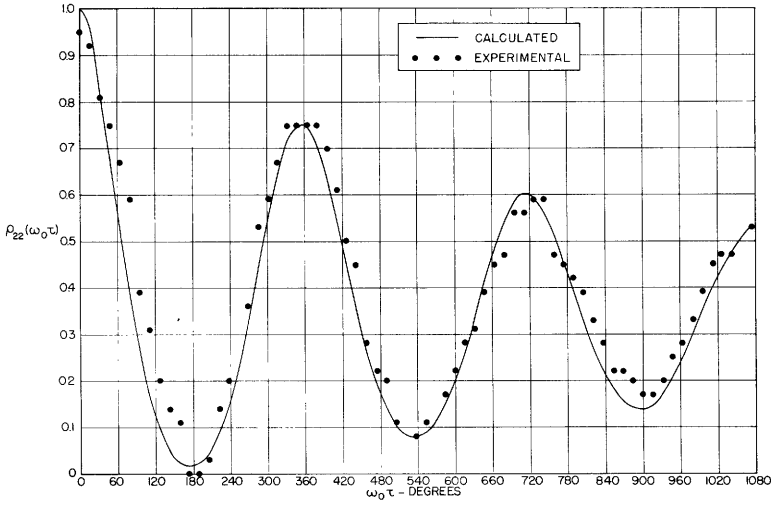

Q = 8.8

Fig. 11 Normalized output autocorrelation functions $\rho_{22}(\omega_0\tau)$ for linear rectifier with a filtered noise input [see Eq. (36)].

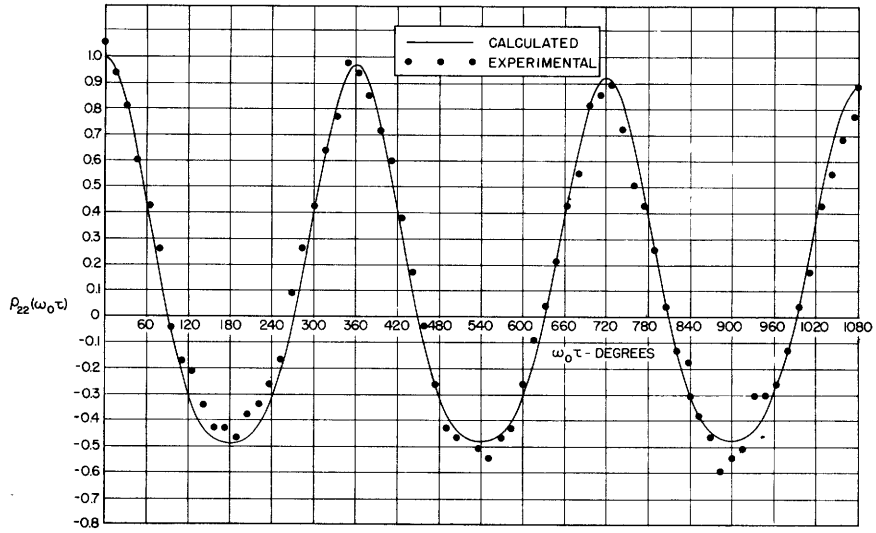

Q = 60

$x = \dfrac{\text{sine wave power}}{\text{noise power}}$

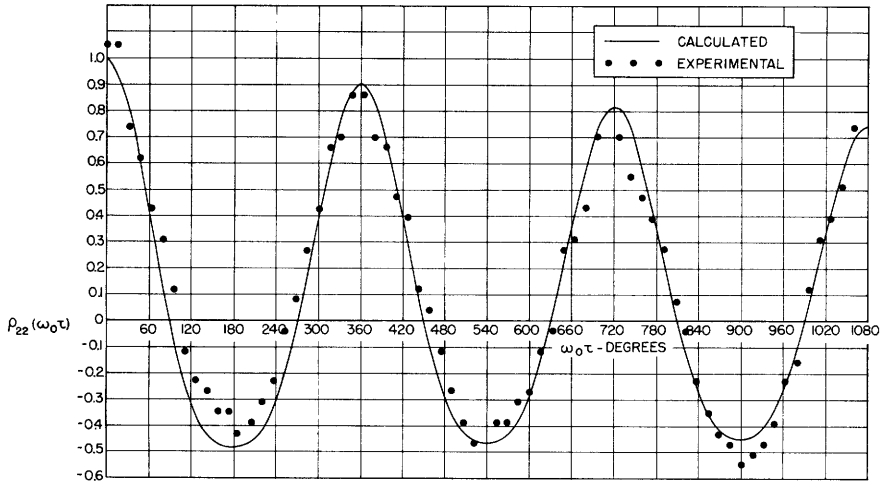

Q = 25

$x = \dfrac{1}{2}$

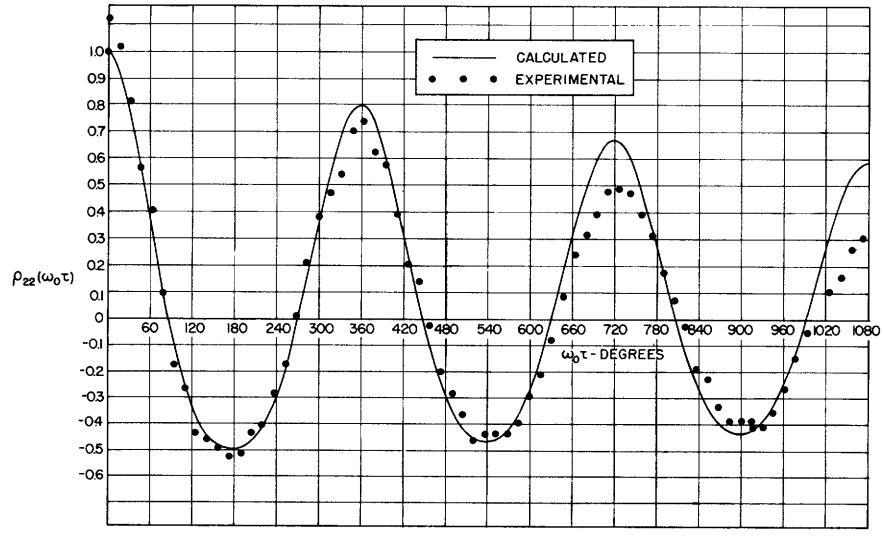

Q = 8.8

x = 1

Fig. 12 Normalized output autocorrelation functions $\rho_{22}(\omega_0\tau)$ for linear rectifier with a filtered noise plus sine wave input [see Eqs. (33), (34), (20)].

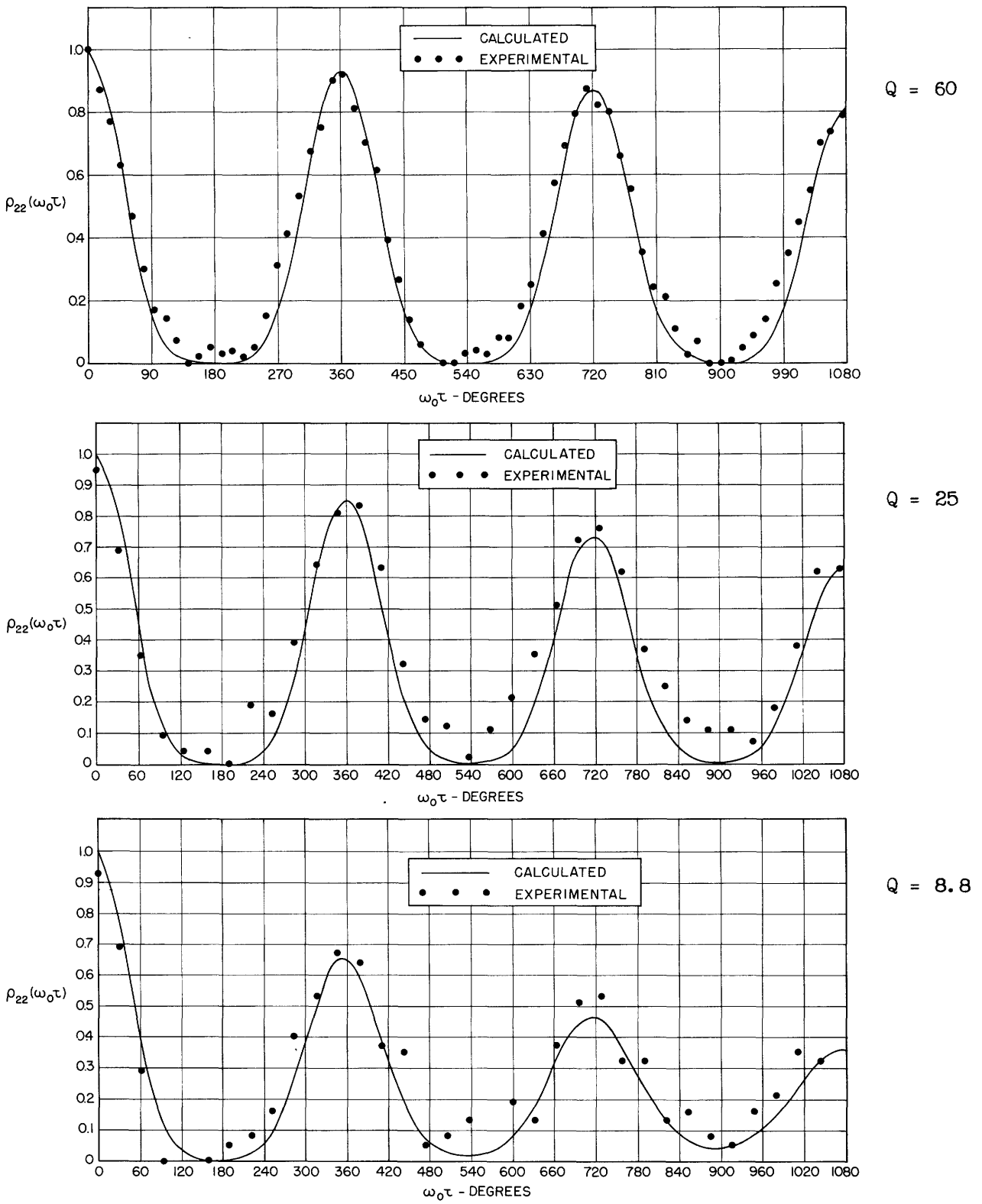

Fig. 13 Normalized output autocorrelation functions $\rho_{22}(\omega_0\tau)$ for square-law rectifier with filtered noise input [see Eq. (37)].

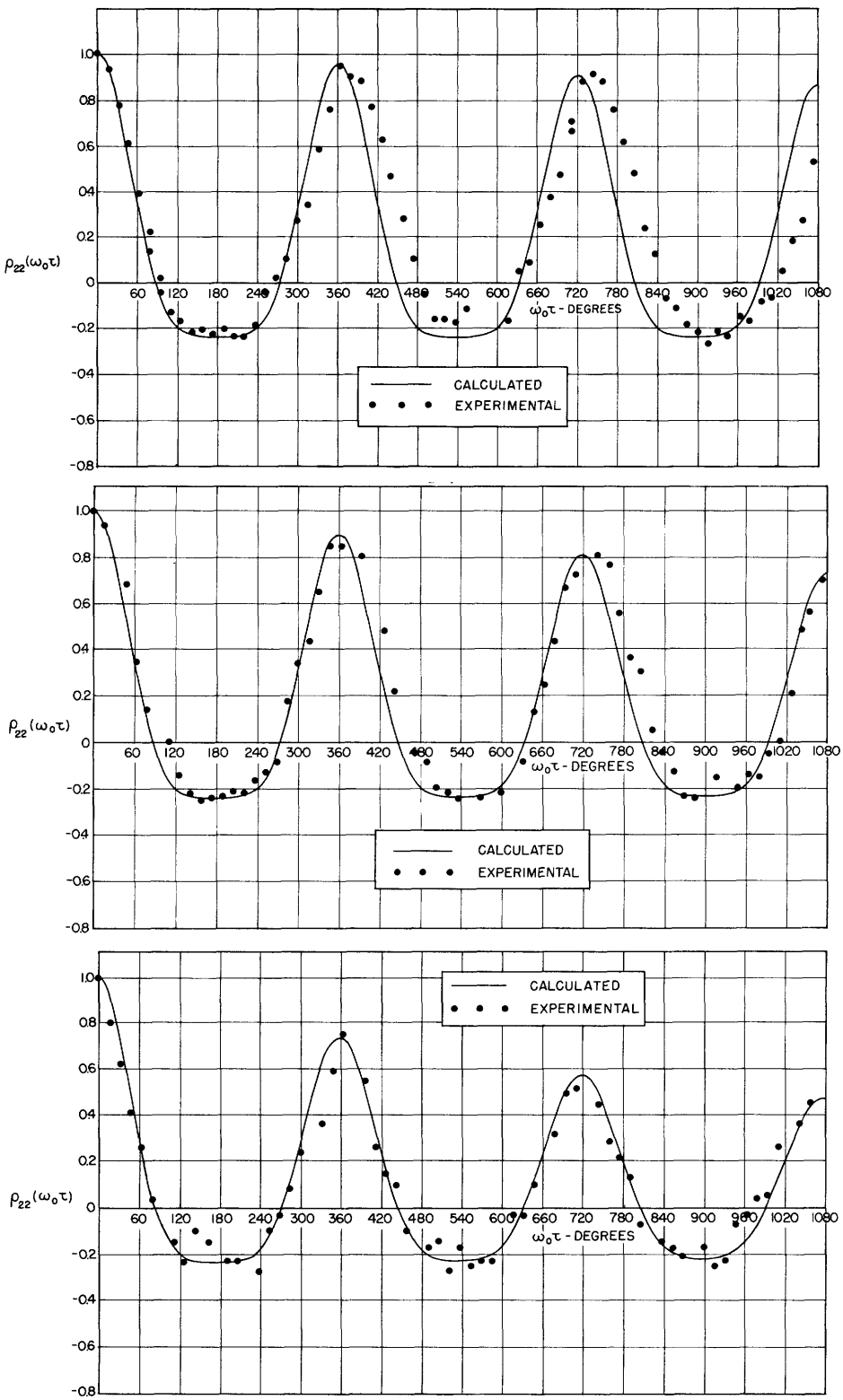

Fig. 14 Normalized output autocorrelation functions $\rho_{22}(\omega_0\tau)$ for square-law rectifier with filtered noise plus sine wave input [see Eqs. (33), (35), (20)].

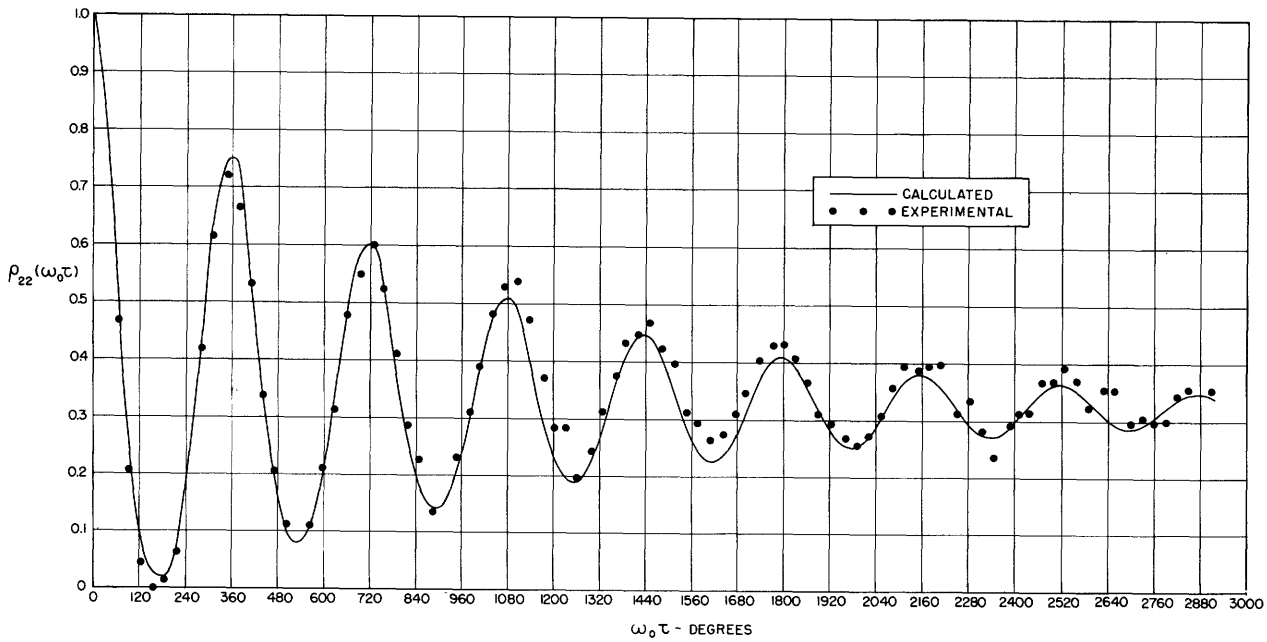

$\rho_{22}(\omega_0\tau)$ for Q = 8.8

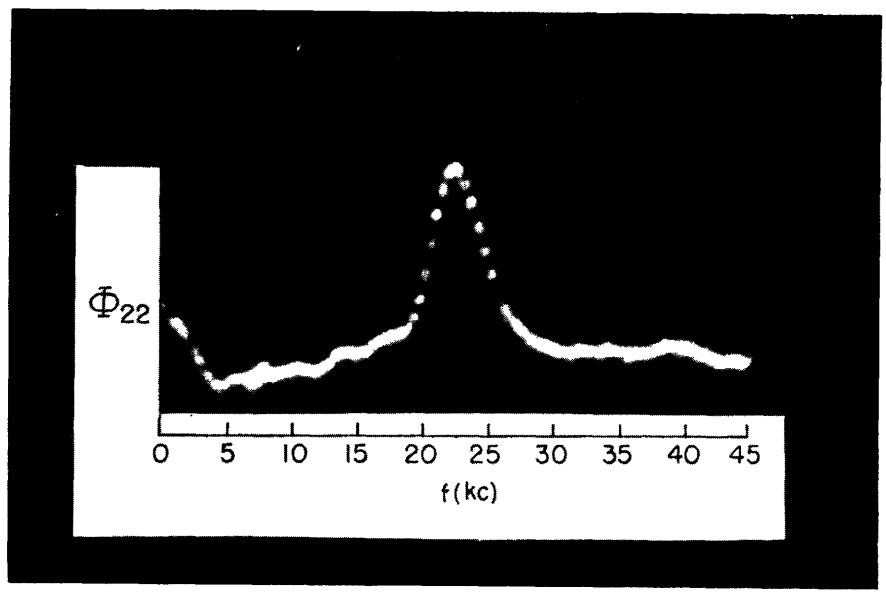

Zeroth and first spectral regions of power density spectrum $\Phi_{22}(\omega)$

Fig. 15 Normalized output autocorrelation function $\rho_{22}(\omega_0\tau)$ for linear rectifier with filtered noise input; and its power density spectrum as obtained on electronic differential analyzer.

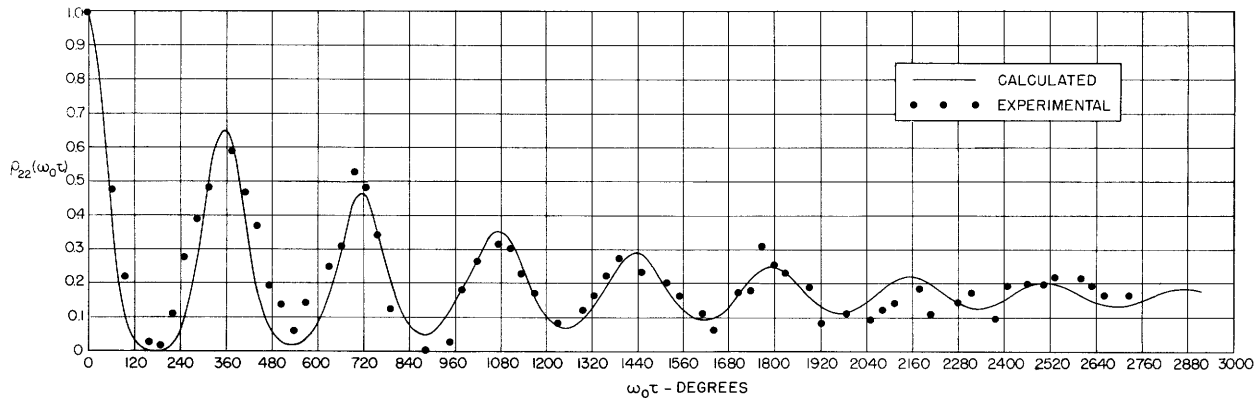

$\rho_{22}(\omega_0\tau)$ for Q = 8.8

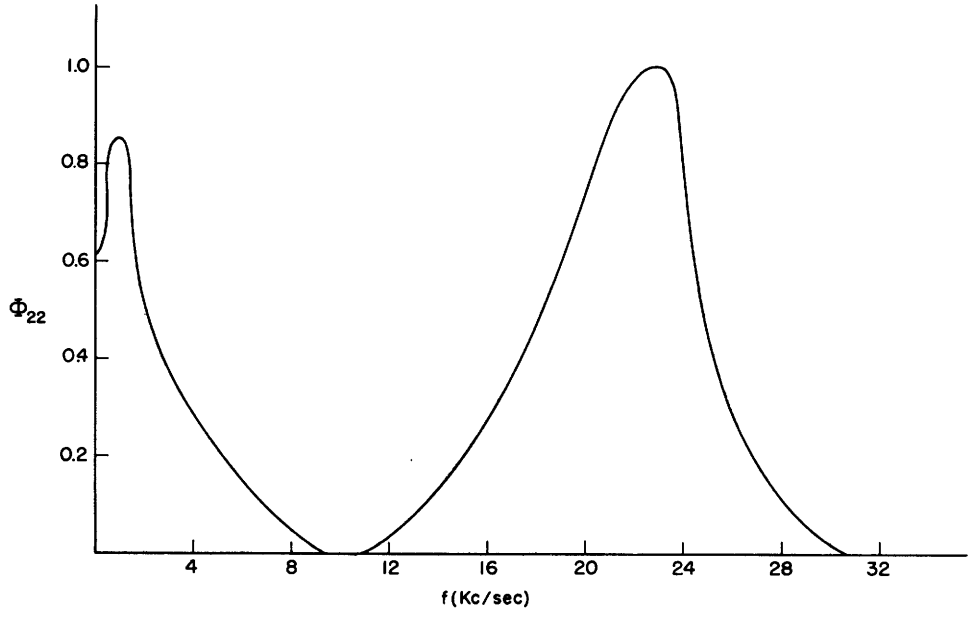

Zeroth and first spectral regions of power density spectrum $\Phi_{22}(\omega)$

Fig. 16 Normalized output autocorrelation function $\rho_{22}(\omega_0\tau)$ for square-law rectifier with filtered noise input; and its power density spectrum as obtained on delay-line filter.

REFERENCES

1. S. O. Rice: Mathematical Analysis of Random Noise, B.S.T.J. 23, pp. 282-332, 1944; 24, pp. 46-156.

2. S. O. Rice: Statistical Properties of a Sine Wave Plus Random Noise, B.S.T.J. 27, pp. 109-157, 1948

3. D. Middleton: The Response of Biased, Saturated Linear and Quadratic Rectifiers to Random Noise, J. App. Phys. 17, No. 10, pp. 778-801, 1946

4. D. Middleton: Some General Results in the Theory of Noise through Nonlinear Devices, Quarterly of Applied Math. 5, pp. 445-498, 1948

5. D. B. Armstrong: A Survey of the Theory of Random Noise; its Behavior in Electronic Circuits, Seminar Paper, Dept. of Elec. Eng. M.I.T. 1950

6. H. E. Singleton: A Digital Electronic Correlator, Technical Report No. 152, Research Laboratory of Electronics, M.I.T. 1950

7. A. B. Macnee: An Electronic Differential Analyzer, Technical Report No. 90, Research Laboratory of Electronics, M.I.T. 1948

8. C. A. Stutt: Experimental Study of Optimum Filters, Technical Report No. 182, Research Laboratory of Electronics, M.I.T. 1951

9. N. Knudtzon: Experimental Study of Statistical Characteristics of Filtered Random Noise, Technical Report No. 115, Research Laboratory of Electronics, M.I.T. July 1949

10. Y. W. Lee: Application of Statistical Methods to Communication Problems, Technical Report No. 181, Research Laboratory of Electronics, M.I.T. Sept. 1950

11. Y. W. Lee, C. A. Stutt: Statistical Prediction of Noise, Technical Report No. 129, Research Laboratory of Electronics, M.I.T. July 1949

12. Gardner and Barnes: Transients in Linear Systems, Vol. I, John Wiley, 1947